Dual-targeting nanomicelles with CD133 and CD44 aptamers for enhanced delivery of gefitinib to two populations of lung cancer-initiating cells

XIAOLONG HUANG[1*], JUN WAN[1*], DEWEN LENG[2*], YINGYING ZHANG[3] and SHUO YANG[1]

Departments of [1]Respiratory Medicine and [2]Critical Care Medicine, Wuhan No. 1 Hospital, Wuhan, Hubei 430022; [3]Department of Pharmacy, Naval Medical University, Shanghai 200433, P.R. China

Abstract. Lung cancer is an aggressive type of cancer that is associated with a high mortality rate. Lung cancer-initiating cells are populations of self-renewing cancer cells with pluripotent differentiation ability. Cancers typically originate from multiple phenotypically distinct cancer-initiating cells. CD133 and CD44 are specific markers that maybe used to distinguish lung cancer-initiating cells. The ability to target a variety of subsets of cancer-initiating cells instead of targeting only one population of cancer initiating-cells has the potential to increase the cancer therapeutic efficacy. In the present study, CD133 and CD44 aptamer-conjugated nano-micelles loaded with gefitinib (CD133/CD44-NM-Gef) were developed to target CD133^{+} and CD44^{+} lung cancer-initiating cells. The therapeutic efficacy of CD133/CD44-NM-Gef against lung cancer-initiating cells was assessed by evaluating cell proliferation, tumorsphere formation and detection of CD44^{+} and CD133^{+} cells using flow cytometry. The results indicated that CD133/CD44-NM-Gef targeted CD133^{+} and CD44^{+} lung cancer-initiating cells and exhibited greater therapeutic efficacy against lung cancer-initiating cells than single-target and non-targeted nanomicelles, suggesting that CD133/CD44-NM-Gef represents a promising treatment for lung cancer by specifically targeting lung cancer-initiating cells. To the best of our knowledge, the present study was the first to report on drug delivery via nanomedicines targeted to multiple populations of cancer-initiating cells using aptamers. As cancer is typically derived from phenotypically distinct cancer-initiating cells, the nanomicelle-based multiple targeting strategy provided is promising for targeting multiple subsets of cancer-initiating cell within a tumor.

Introduction

Lung cancer is one of the most common and aggressive cancer types and is associated with a high mortality rate. It was reported to be a leading cause of cancer-associated death in the US in 2017 (1), and in China, it was the most frequent cause of cancer-associated mortality in males aged ≥75 years in 2015 (2). While numerous advancements have been made in the treatment of lung cancer, therapy failure and low survival rates remain serious issues (3,4). Thus, it is important to develop novel treatments to eliminate lung cancer cells, which are resistant to conventional therapies.

Lung cancer-initiating cells (also called lung cancer stem cells) are considered to be the seeds of lung cancer; they are self-renewing cancer cells with the ability to undergo multi-potential differentiation (5). Treatment resistance and cancer metastasis frequently occur during cancer therapy due to the presence of lung cancer-initiating cells. Therefore, develop-ment of innovative treatments that target and eliminate lung cancer-initiating cells is crucial for improving outcomes for patients with lung cancer. CD133 is a marker for identifying lung cancer-initiating cells (5,6). Previous studies confirmed that CD133^{+} lung cancer cells are able to generate tumori-genic spheres, which were able to initiate tumor growth in mice (5,6). In addition, CD133^{+} lung cancer cells have been indicated to highly express a variety of stemness genes (5,6). A previous study by our group also confirmed that CD133^{+} lung cancer cells expressed high levels of stemness genes and had increased tumorigenicity in mice compared with CD133-lung cancer cells, suggesting that CD133^{+} lung cancer cells exhib-ited lung cancer-initiating cell properties (7). However, tumors may consist of multiple genetically or phenotypically distinct types of cancer-initiating cells. For instance, breast cancer and ovarian cancer contain distinct populations of cancer-initi-ating cells that regenerate the phenotype and heterogeneity of the initial tumor (8,9). In addition to CD133, CD44 is also a specific marker for lung cancer-initiating cells, and CD44^{+} lung cancer cells also have certain properties of stem cells (10). Considering that tumors may consist of heterogeneous

---

Correspondence to: Dr Xiaolong Huang, Department of Respiratory Medicine, Wuhan No. 1 Hospital, 215 Zhongshan Street, Wuhan, Hubei 430022, P.R. China
E-mail: motolongqd@126.com

*Contributed equally

populations of cancer-initiating cells, it was hypothesized that it is imperative to target multiple subsets of cancer-initiating cells to increase the cancer-therapeutic efficacy.

Nanomedicines are characterized by controlled and targeted delivery of drugs and may markedly increase the therapeutic index of common chemotherapy drugs (11). Nanomicelles, a type of nanomedicine prepared by self-assembly of various types of block copolymers, possess several unique features, including simplicity and high efficiency of drug loading (12,13). Polyethylene glycol 2000-distearoyl phosphatidylethanolamine (DSPE-PEG2000) nanomicelles are promising due to their particularly small size (~20 nm), good biocompatibility and superior penetration into solid tumors (14-16). In a previous study by our group, CD133 aptamer-conjugated gefitinib DSPE-PEG2000 nanomicelles (CD133-NM-Gef) were constructed to enhance the delivery of gefitinib into lung tumors (7). In the present study, to achieve simultaneous targeting of nanomicelles to CD44+ and CD133+ cancer cells, CD44 aptamers were further conjugated to CD133-NM-Gef to develop CD133 and CD44 aptamer-conjugated nanomicelles loaded with gefitinib (CD133/CD44-NM-Gef). After characterization of CD133/CD44-NM-Gef, the *in vitro* targeting properties, treatment efficacy and mechanism of action of CD133/CD44-NM-Gef were investigated.

Materials and methods

Culture and passage of lung cancer cells. Two human lung cancer cell lines, namely the H446 small cell lung cancer cell line and the A549 non-small cell lung cancer cell line, were purchased from the American Type Culture Collection. Cells were cultured in RPMI-1640 medium (Thermo Fisher Scientific, Inc.) supplemented with 10% fetal bovine serum (Thermo Fisher Scientific, Inc.) and antibiotics (100 μg/ml streptomycin and 100 U/ml penicillin) at 37°C in 5% CO_2/95% air. The cell culture medium was replaced three times per week and cell maintenance was performed by serial passage after trypsinization.

Lipids, aptamers, antibodies, cytokines and kits. The following lipids were purchased from Avanti Polar Lipids: 1,2-distearoyl-sn-glycero-3-phosphoethanolamine-N-maleimide-PEG-2000 (DSPE-PEG2000-Mal) for sulfhydryl conjugation, 1,2-dioleoyl-sn-glycero-3-phosphoethanolamine-N-carboxyfluorescein (PECF) to label nanomicelles and 1,2-distearoyl-sn-glycero-3-phosphoethanolamine-N- (methoxy PEG2000) (DSPE-PEG2000). Thiolated CD133 aptamers with a sulfhydrylgroup at the 5'-end (5'-SH-CCCUCCUACAUAGGG-3') and thiolated CD44 aptamers with a sulfhydryl group at the 5'-end (5'-SH-GGG AUGGAUCCAAGCUUACUGGCAUCU GGAUUUGCGCGUGCCAGAAUAAAGAGUAUAACGUG UGAAUGGGAAGCUUCGAUAGGAAUUCGG-3') were synthesized and purchased from Ruibo Co., Ltd. Phycoerythrin-labeled CD133 antibodies and Alexa Fluor® 488-labeled CD44 antibodies were purchased from R&D Systems, Inc. The CD133 MicroBead Kits (cat. no. 130-100-857) and CD44 MicroBead Kits (cat. no. 130-095-194) used to isolate CD133+ and CD44+ lung cancer cells were purchased from Miltenyi Biotec. Dalian Meilun Biotech provided gefitinib. Thermo Fisher Scientific, Inc. provided SuperScript III reverse

transcriptase and reagents for culturing lung cancer-initiating cells, including human epidermal growth factor [EGF; freeze-dried powder re-suspended in bovine serum albumin (Thermo Fisher Scientific, Inc.)-containing buffer], human basic fibroblast growth factor (bFGF freeze-dried powder, resuspended in bovine serum albumin-containing buffer), B27 and insulin-transferrin-selenium (ITS). Rat plasma was purchased from Innovative Research, Inc.

Flow cytometry-based analysis of CD133 and CD44 expression and magnetic sorting-based separation. After lung cancer cells were cultured overnight, the cells were trypsinized, washed and suspended in PBS. The cells were then incubated with fluorescent antibody (phycoerythrin-labeled CD133 antibodies; cat. no. FAB11331P-025; and Alexa Fluor® 488-labeled CD44 antibodies; cat. no. FAB6127G; R&D Systems, Inc.) at a final concentration of 1 μg/ml on ice in a refrigerator. After 1 h, the cells were washed with PBS to eliminate any unbound fluorescent antibody. Finally, the washed cells were suspended in PBS for immediate analysis by fluorescence-activated cell sorting (FACS) using a FACSCalibur (BD Biosciences). CD133+ or CD44+ cells were separated using a magnetic column included in the MicroBead kit according to the manufacturer's protocol [CD133 MicroBeadkit (cat. no. 130-100-857) and CD44 MicroBeadkits (cat. no. 130-095-194); both Miltenyi Biotec). The cells were centrifuged and the supernatant was removed. Beads were added and incubated with the cells. Prior to sorting, the column was placed in a magnetic field and rinsed, and the cells were then loaded onto the column. The column was then added to another tube and marker-negative cells were collected. Finally, the proportion of positively-stained cells was analyzed as described above. The rat IgG2B Alexa Fluor® 488-conjugated (cat. no. MAB0061; R&D Systems, Inc.) or phycoerythrin-labeled isotype (cat. no. IC013P; R&D Systems, Inc.) control antibodies with a dilution of 1:500 were used as the negative controls.

In vivo tumorf ormation analysis. The tumor formation assay was performed by inoculating mice with increasing numbers of lung cancer cells. BALB/c nude mice (total number, 240) were purchased from the Shanghai Experimental Animal Center of Chinese Academy of Sciences. All of the mice were 4-5 week-old males weighing ~20 g and housed in a specific pathogen-free environment. All procedures were performed in line with permission from, and within the guidelines of the Animal Administrative Committee of the Naval Medical University (Shanghai, China). The tumor formation assay was performed as follows: Lung cancer cells were washed and re-suspended in PBS. Aliquots of cells (2.5×10^3, 4×10^3, 1×10^4, 2×10^4, 2.5×10^5 and 2.5×10^6 cells, all suspended in 0.1 ml PBS) were completely mixed with BD Matrigel™ (0.1 ml). Then the cell suspension (0.2 ml) was implanted subcutaneously into the right flank of the mice. After implantation, tumor formation in the animals was observed for 15 weeks. Animal health and behavior were monitored once every 3 days during the 15-week period. The mice were euthanized by carbon dioxide inhalation with a flow rate of 2 l/min after 15 weeks or when the tumor volume exceeded 1,500 mm^3. The flow rate of carbon dioxide used for euthanasia of rodents did not displace >30% of the chamber

volume/min. Heartbeat and respiration were checked to verify the death of the mice.

Analysis of tumorsphere formation by lung cancer cells. A tumorsphere is a spherical and solid structure, which is derived from a single cancer stem cell. The tumorsphere formation assay was performed in specific serum-free cell culture medium to assess the self-renewal capability of cancer-initiating cells. In brief, lung cancer cells were cultured overnight and washed to eliminate any residues of medium. The cells were trypsinized, washed and cultured in serum-free cell medium composed of Dulbecco's modified Eagle's medium/F12 (Thermo Fisher Scientific, Inc.), 1X B27, 1X ITS, 0.4% bovine serum albumin, 20 ng/mlEGF and 20 ng/ml bFGF. The cells were then cultured in Corning® ultra-low adherent 6-well dishes (Corning, Inc.) at a density of 5,000 cells/well. The cells were cultured for one week and the number of tumorspheres was calculated by direct observation under a conventional microscope. To obtain second-passage tumorspheres, first-passage tumorspheres were washed and dissociated into single cells using the cell dissociation reagent StemPro®Accutase® (Thermo Fisher Scientific, Inc.). Subsequently, the cells were propagated to form second-passage tumorspheres.

Construction of nanomicelles loaded withgefitinib (NM-Gef). Nanomicelles loaded with gefitinib were constructed using a lipid film-based approach as follows: A total of 2 mg gefitinib and 10 mg of a lipid mixture composed of 8 mg DSPE-PEG2000 and 2 mg DSPE-PEG2000-Mal were dissolved in chloroform. To generate fluorescent nanomicelles, 1% PECF (mass ratio) was added to the lipid mixture. Subsequently, the lipid solution was aspirated and added to a flask, which was then placed on a vacuum rotary evaporator. The lipid mixture was dried completely to obtain a lipid film. The lipid film was then rehydrated by addition of 4 ml PBS. Subsequently, a hand-held extruder (Avanti Polar Lipids) with polycarbonate membranes (100 and 50 nm) was used to obtain small and homogeneous nanomicelles. After preparation of nanomicelles, the following aptamers were incubated with the nanomicelles: CD133 aptamer (0.1 mg), CD44 aptamer (0.1 mg) or CD133 aptamer (0.1 mg) combined with CD44 aptamer (0.1 mg). The mixture was stirred for 4 h. After the reaction, unconjugated aptamers were removed by ultrafiltration using centrifugal filter units (Amicon® Ultra-4, 50 kDa nominal molecular weight limit; EMD Millipore). The following nanomicelles were produced: NM-Gef, CD133-NM-Gef, CD44-NM-Gef, CD133/CD44-NM-Gef and CD133/CD44-NM.

Evaluation of aptamer conjugation efficiency of nanomicelles. After preparation of aptamer-conjugated nanomicelles, the concentration of unconjugated aptamers was measured at 260 nm using an ultraviolet/visible light spectrophotometer. The aptamer conjugation efficiency was calculated using the following formula: Efficiency = $(Q_t-Q_u)/Q_t$, where Q_t is the quantity of total added aptamers and Q_U the quantity of unconjugated aptamers.

Nanomicelle characteristics. After dilution of 100 μl nanomicelles in distilled water (1.9 ml), the diluted samples were placed in sample cells in a Zetasizer Nano ZS90 (Malvern Instruments) to measure the size and zeta potential of the nanomicelles according to a standard protocol. AJEM2100F high-resolution transmission electron microscope (TEM; JEOL Ltd.) was used to visualize the detailed morphology of the phosphotungstic acid-stained nanomicelles.

Reverse-phase high-performance liquid chromatography (HPLC; Agilent 1200L; Agilent Technologies Inc.) was used to determine gefitinib drug loading. In brief, 1 ml of nanomicelle solution was placed in a vacuum oven and completely dried. The dried nanomicelles were dissolved in1 ml methanol for HPLC analysis. A reverse-phase C18 column (Diamonsil®; 250 mm x 4.6 mm, 5 μm particle size; Dikma Technologies, Inc.) was used. The mobile phase consisted of methanol and 0.02 M dipotassium hydrogen orthophosphate 10:90 (v/v) and was maintained at a flow rate of 1.0 ml/min. The detection wavelength of gefitinib was 246 nm. A gefitinib calibration curve was used to determine the gefitinib concentration in the nanomicelles. The drug encapsulation efficacy was determined as the amount of loaded drug divided by the amount of total added drug. The drug loading was calculated as the mass of loaded drug divided by the amount of nanomicelles. A PECF calibration curve was used to determine the PECF concentration in the nanomicelles with BioTek Synergy 4 multimode reader (excitation 495 nm/emission 525 nm; BioTek; Agilent Technologies, Inc.).

Gefitinib release fromn anomicelles. Gefitinib release from nanomicelles was measured in PBS or PBS with 10% rat plasma. The release assay was performed as follows: After the preparation of 5 ml of nanomicelles solution, it was added to a molecular weight cut-off 1,000 Spectra/Por® dialysis membrane (Repligen Corp.). The membrane was sealed and placed in a vessel containing 500 ml release medium. This vessel was placed in a 37°C water bath with gentle stirring at 90 x g using a magnetic stir bar. An aliquot of 0.5 ml dialysate was used for analysis and was replaced with 0.5 ml fresh medium. The amount of gefitinib released was analyzed as described above. The following formula was used to determine gefitinib release: Release rate $= (M_i/M_t) \times 100\%$, where M_i represents the amount of released gefitinib and M_t indicates the total amount of gefitinib.

Flow cytometric analysis of targeting of fluorescent nanomicelles. The targeting of nanomicelles to lung cancer cells was evaluated by flow cytometry. In brief, lung cancer cells were cultured overnight in 10-cm culture plates. The cells were then washed and dissociated into single cells using trypsin. After trypsinization and washing, the cells were cultured at a density of 5×10^5 cells per well on 12-well cell culture plates overnight. After overnight incubation, the old medium was aspirated and replaced with fresh medium. Subsequently, 0.01 ml PECF-labeled nanomicelles (0.5 μg/ml PECF) were prepared and incubated with the cells (5×10^5 cells; 1 ml) at 37°C. After 2 h, the lung cancer cells were trypsinized into single cells and a FACSCalibur flow cytometer was used to analyze the fluorescence of the lung cancer cells.

Effect of nanomicelles on the proliferation of lung cancer cells. Cells in the logarithmic growth phase were seeded in 96-well plates at 3×10^3 cells/well. The plates were incubated
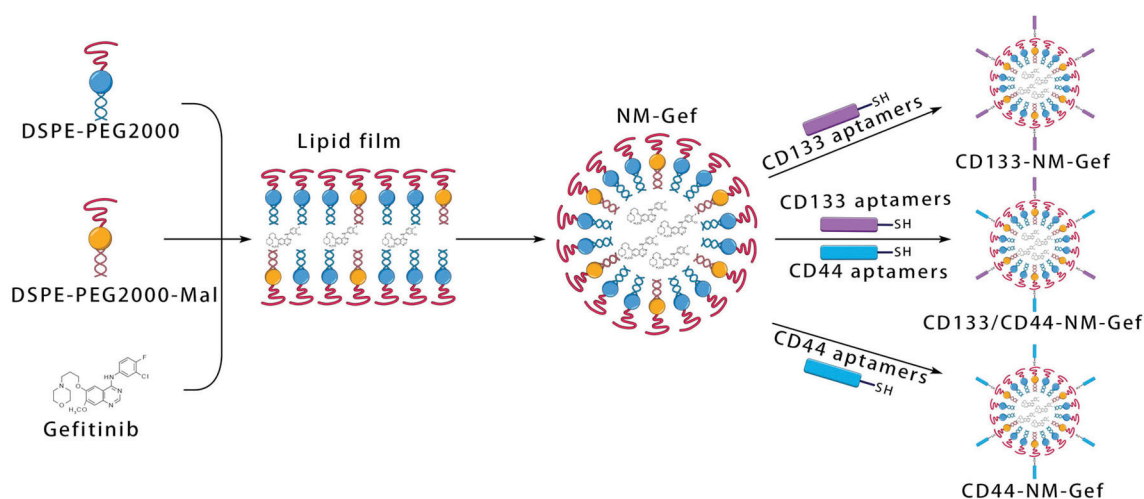
Figure 1. Development of NM loaded with Gef. Gef (2 mg) and lipid mixture (10 mg) were dissolved in chloroform. The lipid chloroform solution was dried to form a lipid film. The dried lipid film was hydrated by addition of PBS. A hand-held extruder was used to generate small NM with good homogeneity. Through reaction of maleimide and sulfhydryl groups, the aptamers were conjugated to the NM. CD133-NM-Gef, CD133 aptamer-conjugated gefitinib DSPE-PEG2000 nanomicelles; DSPE-PEG2000-Mal, 1,2-distearoyl-sn-glycero-3-phosphoethanolamine-N-maleimide-polyethylene glycol-2000.

overnight at 37˚C. After incubation, different concentrations of gefitinib and nanomicelles were added to the wells. The experimental groups were as follows: Gefitinib, NM-Gef, CD133-NM-Gef, CD44-NM-Gef, CD133/CD44-NM-Gef and CD133/CD44-NM. After adding the drug to the wells, the plates were returned to the incubator and cultured for 72 h. Subsequently, the plates were removed from the incubator and 10 μl Cell Counting Kit (CCK)-8 solution was added to each of the wells, taking care not to introduce any bubbles. The plates were returned to the incubator for another 2 h and the absorbance at 450 nm was then measured using a microplate reader (Multiskan MK3; Thermo Fisher Scientific, Inc.). Data were processed with GraphPad Prism 5.0 (GraphPad Software, Inc.) to calculate IC_{50} values.

Tumorsphere assay and flow cytometry-based analysis of the percentages of lung cancer-initiating cells. Tumorsphere assay and flow cytometry-based analysis of the percentages of lung cancer-initiating cells was performed as follows: Lung cancer cell lines containing heterogeneous populations of cells in the logarithmic growth phase were inoculated overnight in 12-well cell culture plates. The cell density was adjusted to $1x10^5$ cells per well and the cells were treated for 24 h with nanomicelles (5 μg/ml equivalent gefitinib concentration) or 5 μg/ml gefitinib dissolved in fresh medium. The groups in this experiment were as follows: NM-Gef, CD133-NM-Gef, CD44-NM-Gef, CD133/CD44-NM-Gef and CD133/CD44-NM. The treatment was terminated by aspiration of the old cell culture medium. Subsequently, the cells were washed with PBS and fresh medium was added. After 72 h, the cells were enzymatically dissociated into single cells and tumorsphere formation was assessed as described above. The cells were cultured in serum-free cell medium in Corning® ultra-low adherence 6-well dishes at a density of 5,000 cells/well. The images of tumorspheres were captured with an EuromexbScope Trinocular Phase Contrast Microscope (Euromex Microscopen bv). Flow cytometry was used to analyze the percentage of CD133+ or CD44+ cells as described above.

Reverse transcription-quantitative (RT-q) PCR. TRIzol reagent (Takara Bio, Inc.) was applied to extract RNA using a standard approach. SuperScript III reverse transcriptase (Thermo Fisher Scientific, Inc.) was used to synthesize first-strand complementary DNA according to the manufacturer's protocol. ASYBR Green PCR kit (cat. no. RR420L; Takara Bio, Inc.) was used to quantify specific transcripts using LightCycler® 1.5 (Roche Applied Science). The following thermocycling conditions were used: Initial denaturation at 95˚C for 10 sec; 40 cycles of 95˚C for 5 sec and 60˚C for 20 sec. The mRNA expression levels, which were normalized against β-actin, were calculated using the $2^{-\Delta\Delta Cq}$ method, as described previously (17). The sequences of the PCR primers were as follows: β-actin forward, 5'-CGTGGACATCCGTAAAG ACC-3' and reverse, 5'-ACATCTGCTGGAAGGTGGAC-3'; CD133 forward, 5'-TCAATTTTGGATTCATATGCCTT-3' and reverse, 5'-ACTCCCATAAAGCTGGACCC-3'; CD44 forward, 5'-TTACAGCCTCAGCAGAGCAC-3' and CD44 reverse, 5'-AAGGACACACCCAAGCAAGG-3'.

Statistical analysis. GraphPad Prism 5.0 (GraphPad Software, Inc., USA) was used for data analysis. Values are expressed as the mean ± standard deviation. Differences between two groups were determined using anunpaired Student's t-test. Differences among three or more groups were determined using one-way analysis of variance with the Newman-Keuls post hoc test. P<0.05 was considered to indicate statistical significance.

Results

Construction, characterization and drug release properties of nanomicelles. Gefitinib-loaded nanomicelles were constructed by lipid film formation, hydration and aptamer conjugation (Fig. 1). Nanomicelles were formed after hydration of the lipid films. To conjugate aptamers to the nanomicelles, the maleimide groups in the nanomicelles were reacted with the sulfhydryl groups in the aptamers. The properties of the nanomicelles are
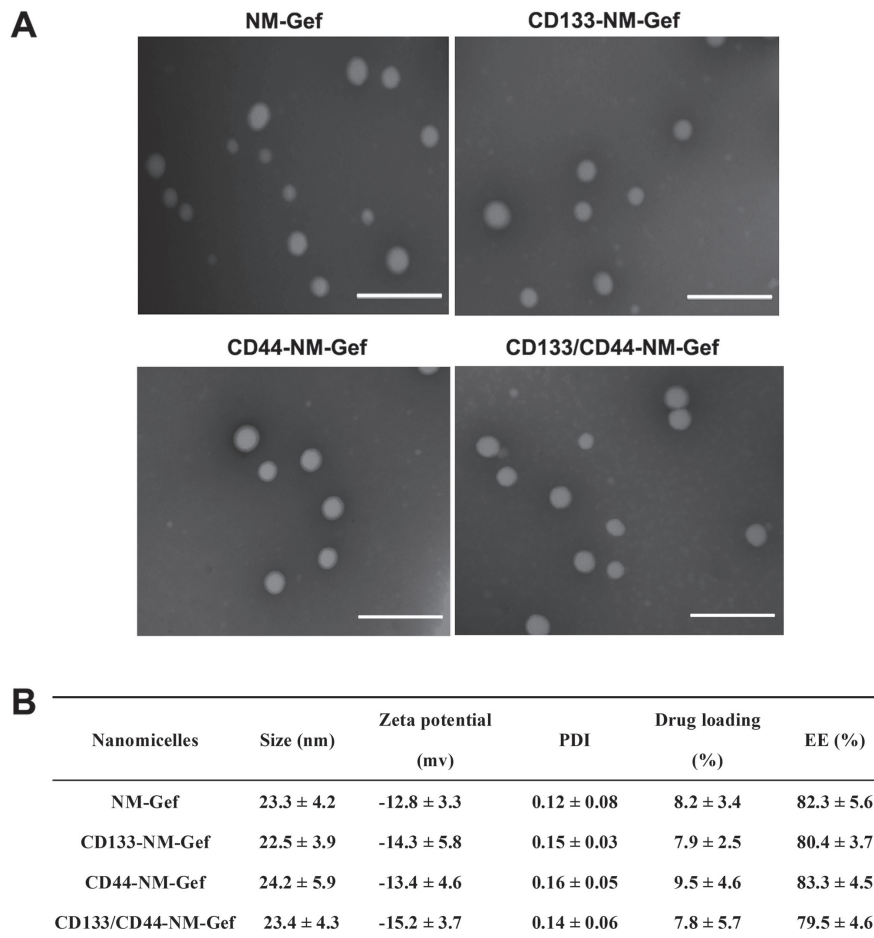
A

B

Nanomicelles	Size (nm)	Zeta potential (mv)	PDI	Drug loading (%)	EE (%)
NM-Gef	23.3 ± 4.2	-12.8 ± 3.3	0.12 ± 0.08	8.2 ± 3.4	82.3 ± 5.6
CD133-NM-Gef	22.5 ± 3.9	-14.3 ± 5.8	0.15 ± 0.03	7.9 ± 2.5	80.4 ± 3.7
CD44-NM-Gef	24.2 ± 5.9	-13.4 ± 4.6	0.16 ± 0.05	9.5 ± 4.6	83.3 ± 4.5
CD133/CD44-NM-Gef	23.4 ± 4.3	-15.2 ± 3.7	0.14 ± 0.06	7.8 ± 5.7	79.5 ± 4.6

Figure 2. Characteristics of various nanomicelles. (A) TEM images of nanomicelles that were negatively stained by PTA. After staining with PTA, the nanomicelles were visualized using TEM at room temperature (scale bars, 100 nm). (B) Size, zeta potential, PDI, drug loading and EE of nanomicelles. Values are expressed as the mean ± standard deviation (n=3). PTA, phosphotungstic acid; TEM, transmission electron microscopy; EE, encapsulation efficiency; PDI, polydispersity index; CD133-NM-Gef, CD133 aptamer-conjugated gefitinib 1,2-distearoyl-sn-glycero-3-phosphoethanolamine-polyethylene glycol-2000 nanomicelles.

summarized in Fig. 2. TEM indicated that all nanomicelles were spherical in shape and uniformly distributed in size (Fig. 2A). As indicated in Fig. 2B, the nanomicelles in each groupwere~20 nm in size with a polydispersity index (PDI) of <0.2. The small size and PDI of the nanomicelles indicated that the nanomicelles prepared were homogeneously distributed. The drug loading of the nanomicelles in each group was 7-9% and the encapsulation efficiency was ~80%, suggesting the nanomicelles efficiently encapsulated gefitinib.

All of the nanomicelles exhibited sustained drug release over a period of 48 h (Fig. 3). Of note, in comparison to gefitinib release in PBS, gefitinib release from the nanomicelles was markedly higher in PBS with plasma (P<0.05). These results may indicate that plasma had the ability to destabilize the structure of the nanomicelles, facilitating the release of gefitinib.

Identification of lung cancer-initiating cells by tumorsphere formation and tumorigenicity assay in mice. After isolation of lung cancer-initiating cells with the MicroBead Kit, the purity of CD133+ or CD44+ cells was determined to be >95%. As indicated in Fig. 4A, the number of first-passage and second-passage tumorspheres of CD44+ H446 cells was markedly greater than that of CD44- H446 cells (P<0.01). In addition, the number of first-passage and second-passage tumorspheres of CD133+ H446 cells was markedly greater than that of CD133- H446 cells (P<0.05; Fig. 4B). For A549 cells, the number of tumorspheres of CD44+ cells was also markedly greater than that of CD44- cells (first-passage tumorspheres: P<0.05; second-passage tumorspheres: P<0.01; Fig. 4C). In summary, the capacity of tumorsphere formation of CD133+ and CD44+ lung cancer cells was markedly greater than that of CD133- and CD44- lung cancer cells.

As presented in (Table I), in the *in vivo* tumor formation experiment, inoculation of ≥2x10⁴ CD133+ H446 cells had a tumor formation rate of 100%. By contrast, for CD133- H446 cells, inoculation of 2x10⁴ cells hada tumor formation rate of onl y10%. Furthermore, CD133- H446 cells induced tumor formation at a rate of 60% when 2.5x10⁶ cells were inoculated. Similar results were obtained for CD133+ and CD133- A549 cells: When the number of cells inoculated was ≥2x10⁴, CD133+ A549 cells had a tumor formation rate of 100%. By contrast, for CD133- A549 cells, 2x10⁴ cells induced tumor formation in 30% of animals. Even at 2.5x10⁶ cells, CD133- H446 cells were only able to achieve a tumor formation rate of 60%. Similarly, the tumorigenicity of
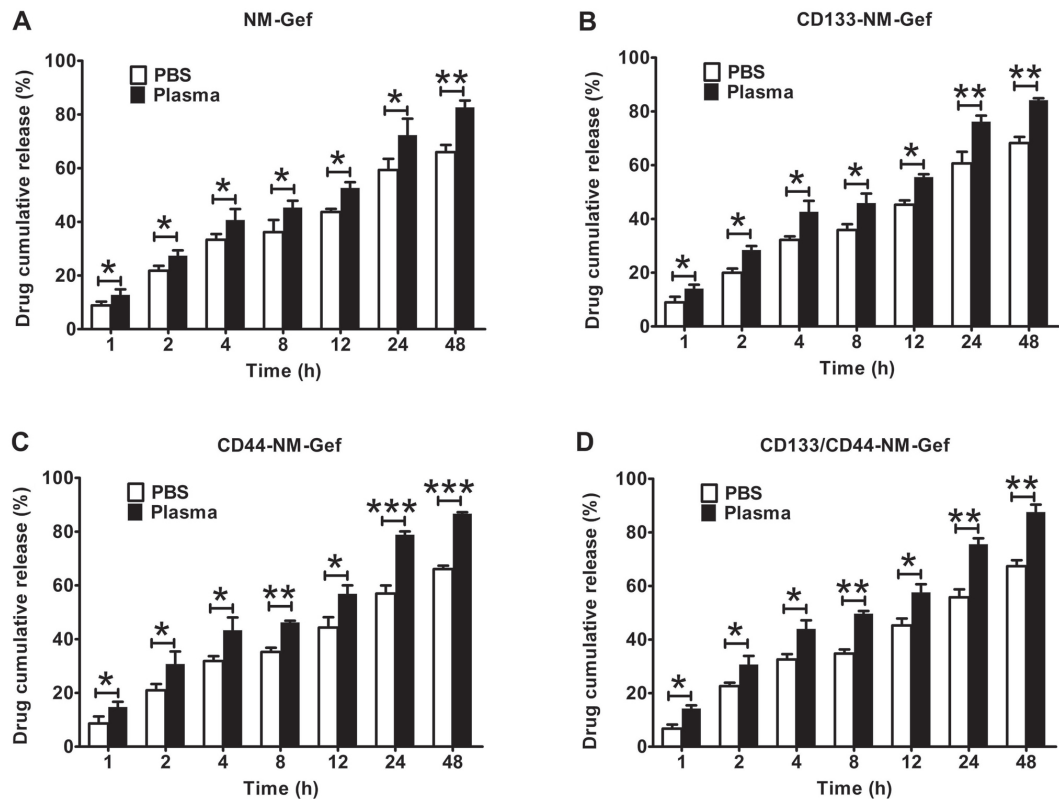
Figure 3. Gefitinib release from nanomicelles. The release medium was PBS or PBS with 10% human plasma. (A) Release of NM-Gef; (B) release of CD133-NM-Gef; (C) release of CD44-NM-Gef; (D) release of CD133/CD44-NM-Gef. Values are expressed as the mean ± standard deviation (n=3). *P<0.05; **P<0.01; ***P<0.001. CD133-NM-Gef, CD133 aptamer-conjugated gefitinib 1,2-distearoyl-sn-glycero-3-phosphoethanolamine-polyethylene glycol-2000 nanomicelles.
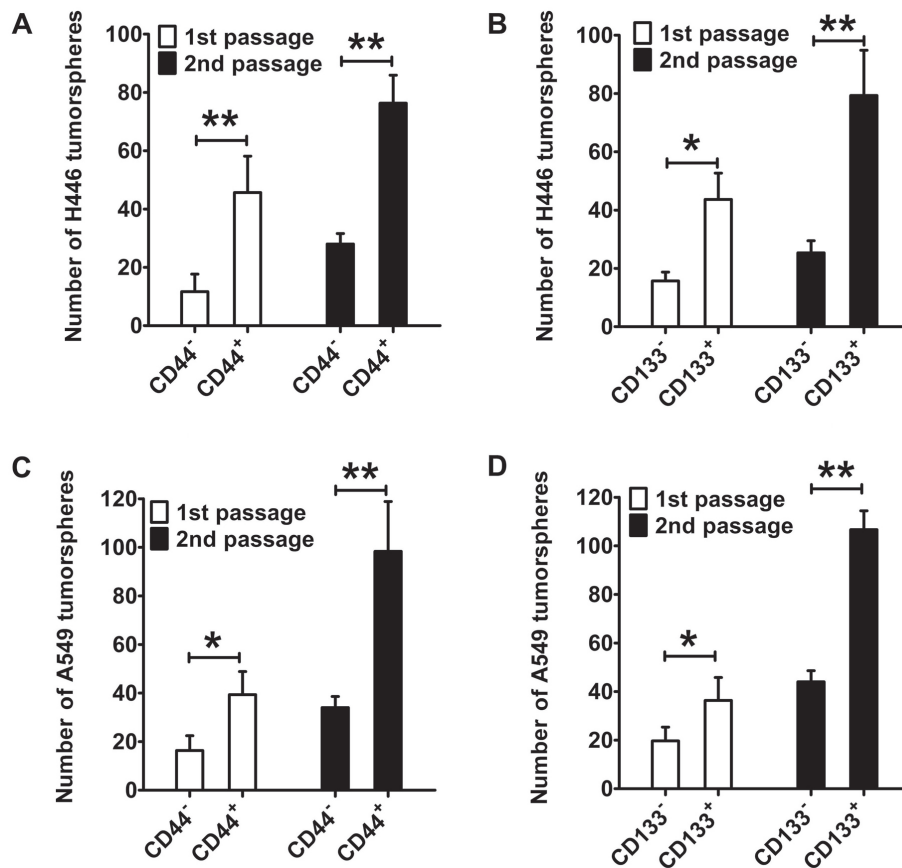

Figure 4. Tumorsphere formation assays. (A) H446 CD44+ and CD44- cells; (B) H446 CD133+ and CD133- cells; (C) A549 CD44+ and CD44- cells; (D) A549 CD133+ and CD133- cells. Values are expressed as the mean ± standard deviation (n=6). *P<0.05, **P<0.01.

Table I. The *in vivo* tumorigenic assay of isolated lung cancer cells based on different markers.

Type	Implanted cell number					
	2.5×10^6	2.5×10^5	2×10^4	1×10^4	4×10^3	2.5×10^3
CD133⁻ H466	6/10	2/10	1/10	0/10	0/10	0/10
CD133⁺ H466	10/10	10/10	10/10	8/10	6/10	5/10
CD133⁻ A549	6/10	3/10	3/10	1/10	0/10	0/10
CD133⁺ A549	10/10	10/10	10/10	9/10	7/10	3/10
CD44⁻ H466	5/10	3/10	2/10	1/10	0/10	0/10
CD44⁺ H466	10/10	9/10	9/10	7/10	5/10	4/10
CD44⁻ A549	7/10	3/10	3/10	2/10	1/10	0/10
CD44⁺ A549	10/10	10/10	8/10	7/10	6/10	3/10

After lung cancer cells were isolated based on different markers (CD44 or CD133), the cells were mixed with Matrigel and implanted subcutaneously into BALB/c nude mice. During an observation period of 15 weeks, the formation of tumors was observed. The number before '/10' indicates the number of mice in which tumors were formed. The maximum diameter exhibited by a single subcutaneous tumor in the present study was 1.6 cm.

CD44⁺ lung cancer cells was greater than that of CD44⁻ lung cancer cells. In the present study, each animal had only one tumor and did not present with multiple tumors.

The tumorsphere assays and tumorigenicity experiments in mice confirmed that CD133⁺ and CD44⁺ cells had characteristics of lung cancer-initiating cells and exhibited a greater tumorigenic ability than CD133⁻ and CD44⁻ cells.

Flow cytometry-based analysis of targeting of fluorescent nanomicelles in vitro. Flow cytometry was used to assess CD133 and CD44 expression in H446 and A549 cells (Fig. 5A and B). In H446 cells, CD44-CD133⁻ cells accounted for >90% of all cells, whereas the percentages of CD44-CD133⁺, CD44⁺CD133⁺ and CD44⁺CD133⁻ cells were <4%. Similar results were obtained for A549 cells, with percentages of CD44⁻CD133⁻, CD44-CD133⁺, CD44⁺CD133⁺ and CD44⁺CD133⁻ cells of 93.1, 2.4, 1.1 and 3.4%, respectively.

Targeting of nanomicelles to lung cancer cells was then evaluated and the results were presented in Fig. 5C-F. PECF-labeled CD133-NM-Gef demonstrated increased targeting to H446 CD133⁺ cells as compared with PECF-labeled NM-Gef (P<0.05; Fig. 5C). Furthermore, PECF-labeled CD133/CD44-NM-Gef exhibited increased targeting to H446 CD133⁺ cells as compared with PECF-labeled NM-Gef and CD44-NM-Gef (P<0.05). However, the targeting efficiency was not markedly different between PECF-labeled NM-Gef, CD133-NM-Gef, CD44-NM-Gef and CD133/CD44-NM-Gef in H446 CD133⁻ cells. In H446 CD44⁺ (Fig. 5D), PECF-labeled CD44-NM-Gef demonstrated increased targeting to H446 CD44⁺ cells as compared with PECF-labeled NM-Gef (P<0.05). Furthermore, PECF-labeled CD133/CD44-NM-Gef exhibited increased targeting to H446 CD44⁺ cells as compared with PECF-labeled NM-Gef and CD133-NM-Gef (P<0.05). However, the targeting efficiency was not markedly different between PECF-labeled NM-Gef, CD133-NM-Gef, CD44-NM-Gef and CD133/CD44-NM-Gef in H446 CD44⁻ cells.

In A549 cells, targeting with nanomicelles was similar to that in H446 cells (Fig. 5E and F). PECF-labeled CD133-NM-Gef exhibited greater targeting to CD133⁺A549 cells than PECF-labeled NM-Gef (P<0.05), and PECF-labeled CD133/CD44-NM-Gef had a greater targeting efficiency toward CD133⁺A549 cells than PECF-labeled NM-Gef and CD44-NM-Gef (P<0.05; Fig. 5E). However, in A549 CD133⁻ cells, the targeting efficiency did not differ significantly among PECF-labeled NM-Gef, CD133-NM-Gef, CD44-NM-Gef and CD133/CD44-NM-Gef. In CD44⁺ A549 cells, PECF-labeled CD44-NM-Gef exhibited a greater targeting efficiency than PECF-labeled NM-Gef (P<0.05), and PECF-labeled CD133/CD44-NM-Gef had a greater targeting efficiency than PECF-labeled NM-Gef and CD133-NM-Gef (P<0.05). However, in CD44-A549 cells, the targeting efficiency did not differ significantly between PECF-labeled NM-Gef, CD133-NM-Gef, CD44-NM-Gef and CD133/CD44-NM-Gef (Fig. 5F).

Effect of nanomicelles on lung cancer cell proliferation. As indicated in Fig. 6, CD133/CD44-NM did not exhibit any toxic effect on lung cancer cells, as evidenced by a zero-slope survival curve. By contrast, gefitinib and gefitinib-loaded nanomicelles produced dose-dependent cytotoxicity toward lung cancer cells. The IC₅₀ values for gefitinib and the nanomicelles are listed in Tables II and III. In H446 CD133⁺ cells, NM-Gef exhibited greater cytotoxicity than gefitinib (33.2±6.4 vs. 73.2±22.5 μg/ml). In addition, CD133/CD44-NM-Gef (6.3±4.3 μg/ml) and CD133-NM-Gef (7.9±4.4 μg/ml) were similarly cytotoxic and were significantly more cytotoxic than NM-Gef (33.2±6.4 μg/ml) and CD44-NM-Gef (31.3±8.5 μg/ml; P<0.01). By contrast, the IC₅₀ values of NM-Gef, CD133-NM-Gef, CD44-NM-Gef, and CD133/CD44-NM-Gef did not differ markedly in H446 CD133⁻ cells, whereas their IC₅₀ was lower than gefitinib. In A549 CD133⁺ cells, CD133/CD44-NM-Gef (5.3±2.8 μg/ml) exerted a greater cytotoxic effect than gefitinib (32.8±8.1 μg/ml), NM-Gef (16.3±7.5 μg/ml) and CD44-NM-Gef (15.4±4.3μg/ml;
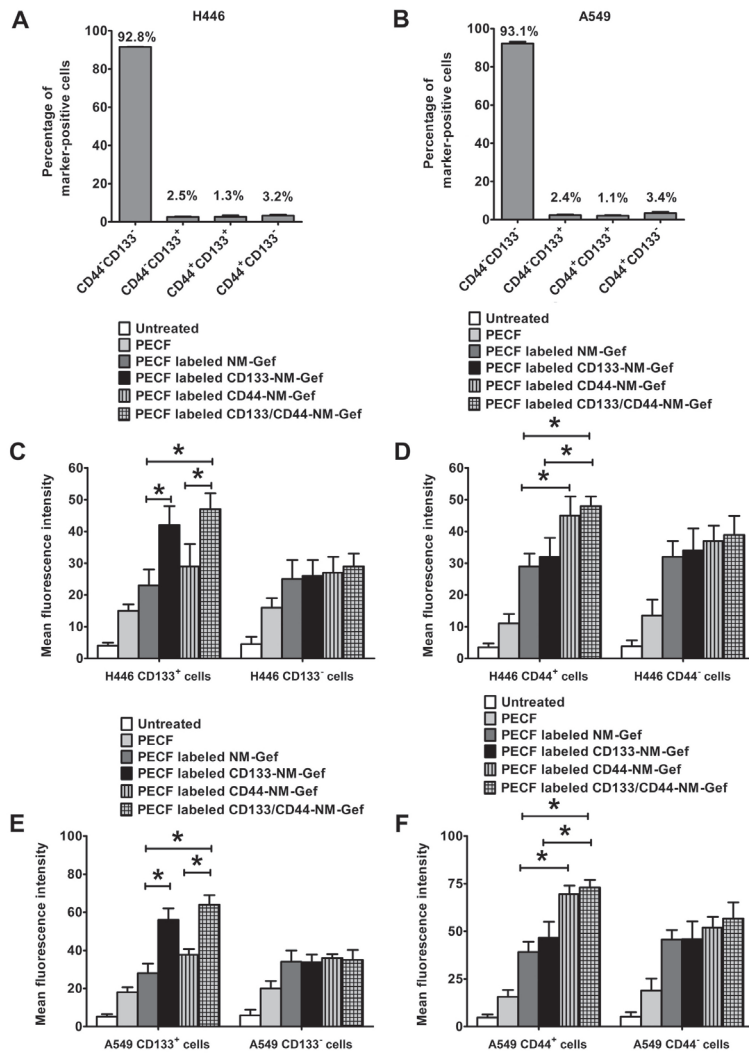
Figure 5. Analysis of CD44 and CD133 expression in lung cancer cells and *in vitro* targeting of fluorescent nanomicelles. (A) Analysis of CD44 and CD133 expression in H446 cells. (B) Analysis of CD44 and CD133 expression in A549 cells. (C) *In vitro* targeting of fluorescent nanomicelles in (C) H446 CD133+ and CD133- cells, (D) H446 CD44+ and CD44- cells, (E) A549 CD133+ and CD133- cells and (F) A549 CD44+ and CD44- cells. Values are expressed as the mean ± standard deviation (n=3). *P<0.05. CD133-NM-Gef, CD133 aptamer-conjugated gefitinib 1,2-distearoyl-sn-glycero-3-phosphoethanolamine-polyethylene glycol-2000 nanomicelles; PECF, 1,2-dioleoyl-sn-glycero-3-phosphoethanolamine-N-carboxyfluorescein.
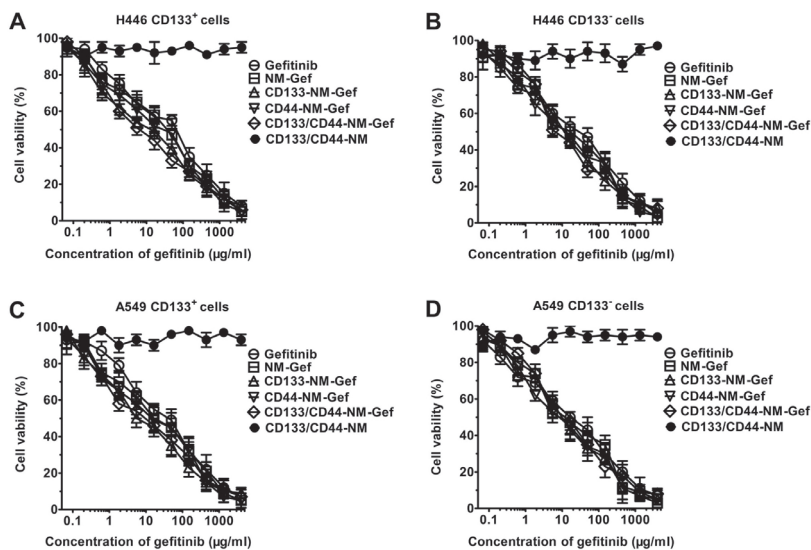

Figure 6. Cell-Counting-Kit-8 assay. (A) H446 CD133+ cells; (B) H446 CD133- cells; (C) A549 CD133+ cells; (D) A549 CD133- cells. Values are expressed as the mean ± standard deviation (n=3).CD133-NM-Gef, CD133 aptamer-conjugated gefitinib 1,2-distearoyl-sn-glycero-3-phosphoethanolamine-polyethylene glycol-2000 nanomicelles.

Table II. IC_{50} values (μg/ml) of gefitinib and nanomicelles in lung cancer cells by CD133 expression status at 72 h.

Treatment	H446		A549	
	CD133$^+$	CD133$^-$	CD133$^+$	CD133$^-$
Gefitinib	73.2±22.5	38.2±6.5	32.8±8.1	15.4±4.3
NM-Gef	33.2±6.4[a]	18.5±8.4	16.3±7.5[a]	12.6±6.4
CD133-NM-Gef	7.9±4.4[c]	16.5±5.8	3.6±2.8[c]	12.1±4.7
CD44-NM-Gef	31.3±8.5	19.5±8.7	15.4±8.4	16.6±7.5
CD133/CD44-NM-Gef	6.3±4.3[b,c]	19.3±6.6	5.3±2.8[b,c]	14.3±6.4
CD133/CD44-NM	>4,000	>4,000	>4,000	>4,000

Values are expressed as the mean ± standard deviation (n=3). [a]P<0.05 vs. gefitinib; [b]P<0.05 vs. NM-Gef; [c]P<0.05CD44-NM-Gef; CD133-NM-Gef, CD133 aptamer-conjugatedgefitinib 1,2-distearoyl-sn-glycero-3-phosphoethanolamine-polyethylene glycol-2000 nanomicelles.

Table III. IC_{50} values (μg/ml) of gefitinib and nanomicelles in lung cancer cells by CD44 expression status at 72 h.

Treatment	H446		A549	
	CD44$^+$	CD44$^-$	CD44$^+$	CD44$^-$
Gefitinib	87.3±15.4	33.3±8.4	44.5±9.5	15.2±7.7
NM-Gef	43.2±8.1[a]	19.4±9.5	21.5±8.5[a]	13.3±8.3
CD133-NM-Gef	38.5±11.4[c]	22.4±6.6	24.4±9.2[c]	19.1±4.3
CD44-NM-Gef	6.3±4.3	23.5±8.4	7.6±4.4	18.8±6.5
CD133/CD44-NM-Gef	5.5±3.5[b]	26.4±5.7	4.1±2.9[b]	21.7±9.5
CD133/CD44-NM	>4,000	>4,000	>4,000	>4,000

Values are expressed as the mean ± standard deviation (n=3). [a]P<0.05 vs. gefitinib; [b]P<0.05 vs. NM-Gef; [c]P<0.05 vsCD44-NM-Gef; CD133-NM-Gef, CD133 aptamer-conjugatedgefitinib 1,2-distearoyl-sn-glycero-3-phosphoethanolamine-polyethylene glycol-2000 nanomicelles.

P<0.01). By contrast, in A549 CD133$^-$ cells, the cytotoxic effect of CD133/CD44-NM-Gef (14.3±6.4 μg/ml) was similar to that of gefitinib (15.4±4.3/ml), NM-Gef (12.6±6.4 μg/ml) and CD44-NM-Gef (16.6 μg/ml). Similar results were obtained in CD44$^+$ and CD44- lung cancer cells (Table II). In summary, CD133/CD44-NM-Gef exerts the most potent cytotoxic effects towards CD133$^+$ and CD44$^+$ lung cancer cells, indicating that CD133/CD44-NM-Gef exhibited dual targeting to CD133$^+$ and CD44$^+$ lung cancer cells. In the future, the cytotoxic effect of gefitinib and nanomicelles on double-positive cells will be investigated.

Percentage of lung cancer-initiating cells as determined by tumorsphere assay and flow cytometry. Treatment with gefitinib and NM-Gef markedly increased the number of H446 tumorspheres (P<0.05; Fig. 7), indicating that gefitinib and NM-Gef exhibited preferential cytotoxic effects toward lung cancer cells but not lung cancer-initiating cells, resulting in an increased percentage of lung cancer-initiating cells. As expected, due to a lack of drug loading, the blank nanomicelles CD133/CD44-NM did not affect the number of tumorspheres generated by H446 cells (Fig. 7A). The inhibitory ability of CD44-NM-Gef and CD133-NM-Gef was greater than that of CD133/CD44-NM (P<0.01). Of note, CD133/CD44-NM-Gef treatment exerted greater inhibitory effects than CD44-NM-Gef and CD133-NM-Gef (P<0.05). Similarly, in A549 cells, CD133/CD44-NM-Gef treatment inhibited tumorsphere formation to the greatest extent (Fig. 7B). Representative images of tumorspheres are provided in Fig. 7C and D.

Consistent results were obtained by flow cytometric analysis of the percentage of CD44$^+$ or CD133$^+$ H446 and A549 cells (Fig. 8A-D). In H446 cells, the percentage of CD44$^+$ cells was markedly increased after gefitinib and NM-Gef treatment (P<0.05) and was markedly decreased after treatment with CD44-NM-Gef or CD133/CD44-NM-Gef (P<0.05; Fig. 8A). For A549 CD44$^+$ cells, similar results were obtained (Fig. 8B). The percentage of CD133$^+$ H446 cells was markedly increasedafter treatment with gefitinib orNM-Gef (P<0.05; Fig. 8C). CD133-NM-Gef and CD133/CD44-NM-Gef exerted similar inhibitory effects on the percentage of CD133$^+$ H446 cells. For CD133$^+$ A549 cells, similar results were obtained (Fig. 8D). Representative flow cytometric images are provided in Fig. S1. In general, the proportion of marker-positive cancer stem cells in cancer cell lines is low. In line with this, Fig. S1 indicated that the majority
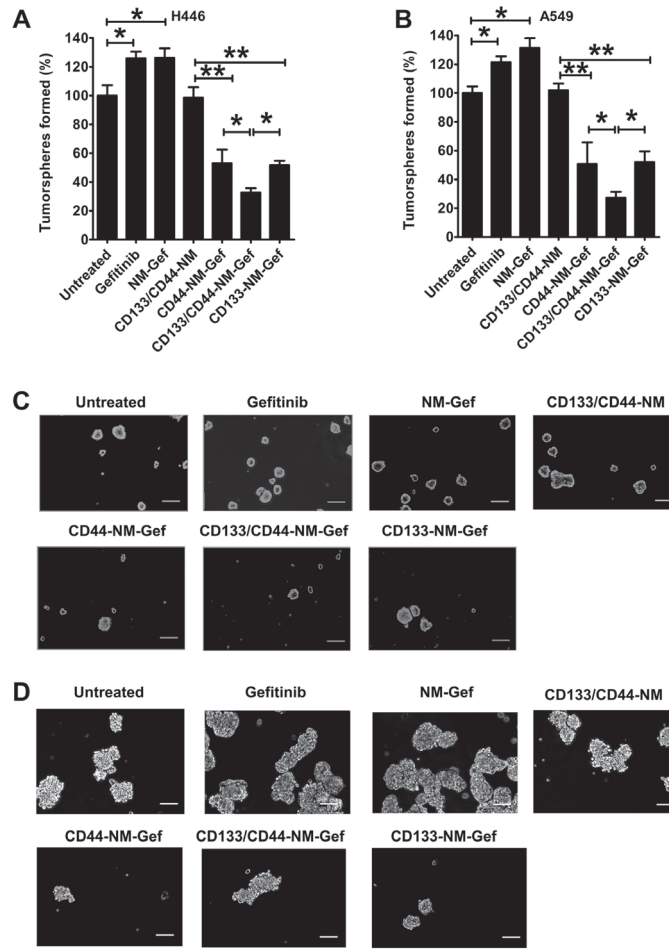
Figure 7. Effect of nanomicelles on the tumorsphere formation in H446 and A549 cells. (A and B) Quantitative results of tumorsphere formation relative to the untreated group. Values are expressed as the mean ± standard deviation (n=6). (C and D) Representative images of the tumorsphere formation of (C) H446 and (D) A549 cells (scale bars, 100 μm).*P<0.05, **P<0.01. CD133-NM-Gef, CD133 aptamer-conjugated gefitinib 1,2-distearoyl-sn-glycero-3-phosphoethanol-amine-polyethylene glycol-2000 nanomicelles.
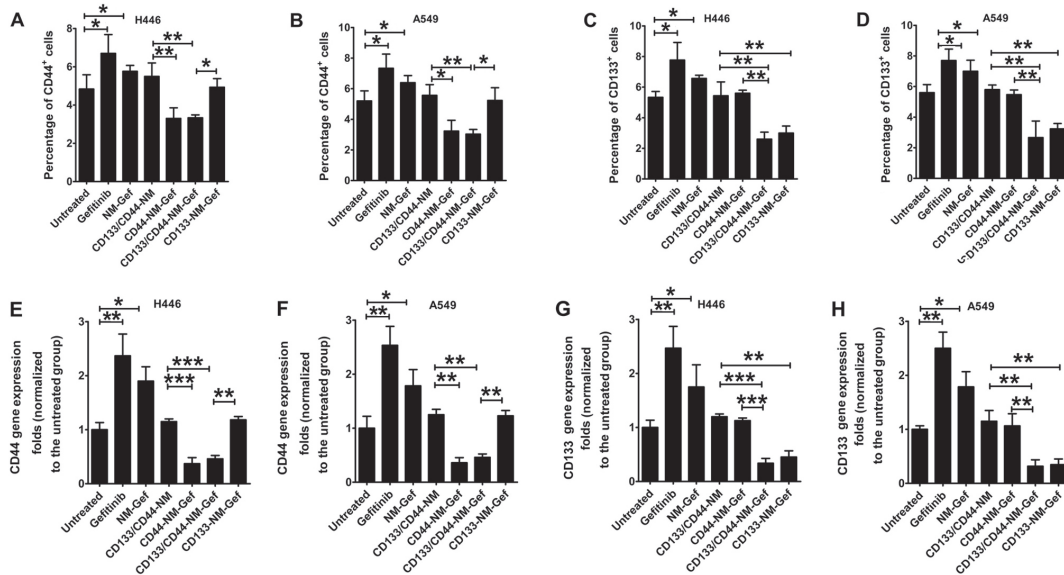

Figure 8. Effect of nanomicelles on the percentage of lung cancer-initiating cells and and associated gene expression. (A-D) Effect of nanomicelles on the percentage of lung cancer-initiating cells. (E-H) Effect of nanomicelles on the gene expression associated with lung cancer-initiating cells. The mRNA expression of CD44 and CD133 in H446 and A549 cells was detected by reverse transcription-quantitative PCR. Each value represents the relative ratio of the respective experimental group to the untreated group. Values are expressed as the mean ± standard deviation (n=6). *P<0.05, **P<0.01, ***P<0.001. CD133-NM-Gef, CD133 aptamer-conjugated gefitinib 1,2-distearoyl-sn-glycero-3-phosphoethanolamine-polyethylene glycol-2000 nanomicelles.
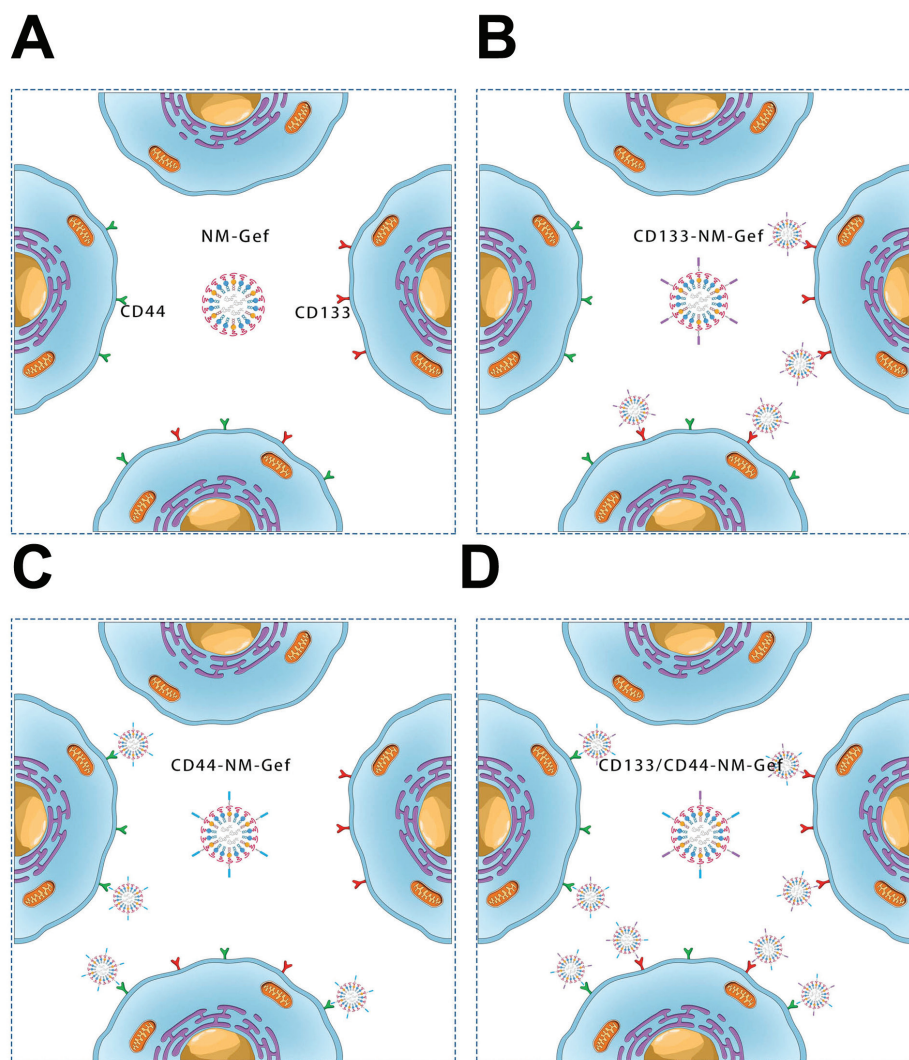
Figure 9. Mechanismsof targeting of thefour different nanomicelles towards lung cancer cells. (A) NM-Gef did not specifically target any subgroups of lung cancer cells. (B) CD133-NM-Gef only targeted CD44+CD133+ cells and CD44-CD133+ cells. (C) CD44-NM-Gef only targeted CD44+CD133+ cells and CD44+CD133- cells. (D) CD133/CD44-NM-Gef targeted CD44+CD133+ cells, CD44+CD133- and CD44- CD133+ cells. CD133-NM-Gef, CD133 aptamer-conjugated gefitinib 1,2-distearoyl-sn-glycero-3-phosphoethanolamine-polyethylene glycol-2000 nanomicelles.

of the cells were negative for these markers. In summary, CD133/CD44-NM-Gef decreased the percentages of CD133+ and CD44+ lung cancer-initiating cells, indicating better therapeutic efficacy toward lung cancer-initiating cells than CD44-NM-Gef and CD133-NM-Gef. The RT-qPCR analysis results of mRNA expression of CD44 and CD133 in H446 and A549 cells indicated similar trends to the flow cytometry results (Fig. 8E-H).

Discussion

Targeting and elimination of lung cancer-initiating cells, which are considered the seeds of lung cancer, may be able to effectively eradicate lung cancer. Int he present study, CD133/CD44-NM-Gef was developed to target CD133+ and CD44+ lung cancer-initiating cells. CD133/CD44-NM-Gef was demonstrated to target CD133+ and CD44+ lung cancer-initiating cells and exhibited a better therapeutic efficacy toward lung cancer-initiating cells in comparison to single-target and non-targeted nanomicelles, suggesting that

CD133/CD44-NM-Gef represents a promising treatment for lung cancer-initiating cells.

The safety of nanomedicines is a critical factor for determining their suitability for clinical application (18). Inorganic nanomedicines, including silicon or noble metal nanoparticles, in contrast to biodegradable organic nanomicelles, do not undergo degradation (18). Since biodegradable organic nanomedicines exhibit superior biocompatibility and safety, they offer a more promising strategy for clinical use (18-20). In the present study, the components of CD133/CD44-NM-Gef included gefitinib, DSPE-PEG2000 and aptamers. Gefitinib, which was initially heralded as a breakthrough in lung cancer therapy, was approved by the US Food and Drug Administration (FDA) as the first tyrosine kinase inhibitor (TKI) for lung cancertherapy (21). DSPE-PEG2000 is an FDA-approved lipid material and has been widely used for the preparation of various long-circulation liposomes. Aptamers are oligonucleotide molecules that bind to a specific target, and pegaptanib, a targeted anti-vascular endothelial growth factor aptamer, has been FDA-approved for intraocular injection for

the treatment of ocular vascular diseases (22). The cytotoxicity assays in the present study demonstrated that the blank drug delivery system did not induce toxicity *in vitro.*

Several chemotherapy drugs, including salinomycin and metformin, have been demonstrated to eliminate cancer-initiating cells (23). Several studies have previously confirmed the selective activity of salinomycin toward cancer-initiating cells (24-26). Although several clinical pilot studies initially confirmed the potent activity of salinomycin toward therapy-resistant cancers, it is highly toxic and has a narrow therapeutic window (27). In addition, there are no FDA-approved chemotherapeutic drugs for targeting cancer-initiating cells. Thus, the present study aimed to construct a novel drug delivery system to target cancer-initiating cells. Although gefitinib was the first approved TKI for lung cancer, the present results indicated that it markedly increased tumorsphere formation and the percentage of CD44+ and CD133+ cells, indicating that lung cancer-initiating cells are resistant to gefitinib. However, CD133/CD44-NM-Gef targeted CD133+ and CD44+ lung cancer-initiating cells, suggesting that CD133/CD44-NM-Gef may overcome the resistance of lung cancer-initiating cells to gefitinib and demonstrating the therapeutic potential of these nanomicelles. As indicated by Gao et al (23), nanomedicines may be able to eradicate cancer-initiating cells by utilizing cancer-initiating cell phenotype-specific ligands to deliver drugs to these cells.

Ligand-conjugated nanomedicines are promising agents for cancer therapy, as they have the ability to markedly increase therapeutic effects (20,28). Of note, two ligand-conjugated nanomedicines (doxorubicin- or docetaxel-loaded nanomedicines) have undergone successful clinical trials for safety and efficacy (29,30). In the present study, the CD133 and CD44 aptamers were demonstrated to be crucial for specific targeting of CD133/CD44-NM-Gef to CD133+ and CD44+ lung cancer-initiating cells. In CD133+ and CD44+ lung cancer-initiating cells, CD133/CD44-NM-Gef demonstrated markedly enhanced targeting compared with single-target and non-targeted nanomicelles, resulting in enhanced therapeutic effects. It was therefore proven that CD44 and CD133 aptamers promoted targeting of nanomicelles to lung cancer-initiating cells. To the best of our knowledge, the present study was the first to investigate the promotion of drug delivery via nanomedicines to multiple populations of cancer-initiating cells using aptamers. Considering that tumors consist of multiple phenotypically distinct types of cancer-initiating cell, the present nanomicelle-based multiple targeting strategy is promising for targeting multiple subsets of cancer-initiating cells within a tumor to increase the therapeutic efficacy.

The present study also elucidated the mechanisms underlying the superior anticancer efficacy of CD133/CD44-NM-Gef toward lung cancer-initiating cells (Fig. 9). NM-Gef did not specifically target any cell population due to the absence of CD44 or CD133 aptamers. By contrast, CD133-NM-Gef exhibited enhanced targeting to CD44+/CD133+ and CD44-/CD133+ cells, whereas CD44-NM-Gef exhibited enhanced targeting to CD44+/CD133+ and CD44+/CD133- cells, suggesting that CD133-NM-Gef and CD44-NM-Gef could show enhanced targeting of CD44+/CD133+ cells or single positive cells (CD44 or CD133) than NM-Gef. Of note, targeting of CD133/CD44-NM-Gef to CD44+/CD133+, CD44+/CD133- and

CD44-/CD133+ cells in the whole cell population was enhanced due to conjugation of the two aptamers. Although combination of CD133-NM-Gef + CD44-NM-Gef may achieve the same effect as CD133/CD44-NM-Gef, administration of one drug may be feasible than the combination of two nanoparticles (26). The present study demonstrated that CD133/CD44-NM-Gef exerted a significantly greater therapeutic efficacy toward CD44+ and CD133+ lung cancer-initiating cells than nanomicelles that did not contain any aptamers.

One limitation of the present study was that no clone formation assay was performed in the present study to further confirm the effect of the drugs on lung cancer-initiating cells (25). The tumorsphere assay in our study was used to evaluate the effects of drugs on cell renewal ability. In future experiments, the clone formation assay will be performed to substantiate the results obtained in the present study. Another limitation is that the cytotoxic effects of drugs on double-positive cells, single-positive/single-negative cells have not been evaluated, and experiments to evaluate the cytotoxic effects of drugs on double-positive cells should be performed in the future.

In conclusion, the present study was the first to demonstrate targeted drug delivery via nanomicelles to three populations of cancer-initiating cells using aptamers, to the best of our knowledge. CD133/CD44-NM-Gef represents a promising agent for the treatment of lung cancer by targeting cancer-initiating cells. Considering that eradication of lung cancer-initiating cells is crucial for improving the therapeutic efficacy of lung cancer treatments, patients with lung cancer may substantially benefit from this dual-targeted therapeutic approach to treat three populations of lung cancer-initiating cells.

Acknowledgements

Funding

Availability of data and materials

All data generated or analyzed during this study are included in this published article.

Authors' contributions

XH, JW and DL contributed to the design of the study and wrote the manuscript. DL and YZ performed the experiments. SY analyzed the data. All authors have read and approved the manuscript.

Ethics approval and consent to participate

The animal experimental protocols were approved by the Animal Administrative Committee of the Naval Medical University (Shanghai, China).

Patient consent for publication

Not applicable.

Competing interests

The authors declare that they have no competing interests.

References

1. Siegel RL, Miller KD and Jemal A: Cancer Statistics, 2017. CA Cancer J Clin 67: 7-30, 2017.
2. Chen W, Zheng R, Baade PD, Zhang S, Zeng H, Bray F, Jemal A, Yu XQ and He J: Cancer statistics in China, 2015. CA Cancer J Clin 66: 115-132, 2016.
3. Eramo A, Lotti F, Sette G, Pilozzi E, Biffoni M, Di Virgilio A, Conticello C, Ruco L, Peschle C and De Maria R: Identification and expansion of the tumorigenic lung cancer stem cell population. Cell Death Differ 15: 504-514, 2008.
4. Kim JJ and Tannock IF: Repopulation of cancer cells during therapy: An important cause of treatment failure. Nat Rev Cancer 5: 516-525, 2005.
5. Zakaria N, Satar NA, Abu Halim NH, Ngalim SH, Yusoff NM, Lin J and Yahaya BH: Targeting lung cancer stem cells: Research and clinical impacts. Front Oncol 7: 80, 2017.
6. Bertolini G, Roz L, Perego P, Tortoreto M, Fontanella E, Gatti L, Pratesi G, Fabbri A, Andriani F, Tinelli S, et al: Highly tumorigenic lung cancer CD133+ cells display stem-like features and are spared by cisplatin treatment. Proc Natl Acad Sci USA 106: 16281-16286, 2009.
7. Huang X, Huang J, Leng D, Yang S, Yao Q, Sun J and Hu J: Gefitinib-loaded DSPE-PEG2000 nanomicelles with CD133 aptamers target lung cancer stem cells. World J Surg Oncol 15: 167, 2017.
8. Meyer MJ, Fleming JM, Lin AF, Hussnain SA, Ginsburg E and Vonderhaar BK: CD44posCD49fhiCD133/2hi defines xenograft-initiating cells in estrogen receptor-negative breast cancer. Cancer Res 70: 4624-4633, 2010.
9. Stewart JM, Shaw PA, Gedye C, Bernardini MQ, Neel BG and Ailles LE: Phenotypic heterogeneity and instability of human ovarian tumor-initiating cells. Proc Natl Acad Sci USA 108: 6468-6473, 2011.
10. Leung EL, Fiscus RR, Tung JW, Tin VP, Cheng LC, Sihoe AD, Fink LM, Ma Y and Wong MP: Non-small cell lung cancer cells expressing CD44 are enriched for stem cell-like properties. PLoS One 5: e14062, 2010.
11. Jain RK and Stylianopoulos T: Delivering nanomedicine to solid tumors. Nat Rev Clin Oncol 7: 653-664, 2010.
12. Li W, Li J, Gao J, Li B, Xia Y, Meng Y, Yu Y, Chen H, Dai J, Wang H, et al: The fine-tuning of thermosensitive and degradable polymer micelles for enhancing intracellular uptake and drug release in tumors. Biomaterials 32: 3832-3844, 2011.
13. Li W, Zhao H, Qian W, Li H, Zhang L, Ye Z, Zhang G, Xia M, Li J, Gao J, et al: Chemotherapy for gastric cancer by finely tailoring anti-Her2 anchored dual targeting immunomicelles. Biomaterials 33: 5349-5362, 2012.
14. Ashok B, Arleth L, Hjelm RP, Rubinstein I and Onyüksel H: In vitro characterization of PEGylated phospholipid micelles for improved drug solubilization: Effects of PEG chain length and PC incorporation. J Pharm Sci 93: 2476-2487, 2004.
15. Zhao BJ, Ke XY, Huang Y, Chen XM, Zhao X, Zhao BX, Lu WL, Lou JN, Zhang X and Zhang Q: The antiangiogenic efficacy of NGR-modified PEG-DSPE micelles containing paclitaxel (NGR-M-PTX) for the treatment of glioma in rats. J Drug Target 19: 382-390, 2011.
16. Mao X, Liu J, Gong Z, Zhang H, Lu Y, Zou H, Yu Y, Chen Y, Sun Z, Li W, et al: iRGD-conjugated DSPE-PEG2000 nanomicelles for targeted delivery of salinomycin for treatment of both liver cancer cells and cancer stem cells. Nanomedicine (Lond) 10: 2677-2695, 2015.
17. Livak KJ and Schmittgen TD: Analysis of relative gene expression data using real-time quantitative PCR and the 2 (-Delta Delta C (T)) Method. Methods 25: 402-408, 2001.
18. Cushing BL, Kolesnichenko VL and O'Connor CJ: Recent advances in the liquid-phase syntheses of inorganic nanoparticles. Chem Rev 104: 3893-3946, 2004.
19. Gao J, Ochyl LJ, Yang E and Moon JJ: Cationic liposomes promote antigen cross-presentation in dendritic cells by alkalizing the lysosomal pH and limiting degradation of antigens. J Nanomedicine 12: 1251-1264, 2017.
20. Gao J, Chen H, Song H, Su X, Niu F, Li W, Li B, Dai J, Wang H and Guo Y: Antibody-targeted immunoliposomes for cancer treatment. Mini Rev Med Chem 13: 2026-2035, 2013.
21. Passiglia F, Listì A, Castiglia M, Perez A, Rizzo S, Bazan V and Russo A: EGFR inhibition in NSCLC: New findings and opened questions? Crit Rev Oncol Hematol 112: 126-135, 2017.
22. Ng EW, Shima DT, Calias P, Cunningham ET Jr, Guyer DR and Adamis AP: Pegaptanib, a targeted anti-VEGF aptamer for ocular vascular disease. Nat Rev Drug Discov 5: 123-132, 2006.
23. Gao J, Li W, Guo Y and Feng SS: Nanomedicine strategies for sustained, controlled and targeted treatment of cancer stem cells. Nanomedicine (Lond) 11: 3261-3282, 2016.
24. Gong Z, Chen D, Xie F, Liu J, Zhang H, Zou H, Yu Y, Chen Y, Sun Z, Wang X, et al: Codelivery of salinomycin and doxorubicin using nanoliposomes for targeting both liver cancer cells and cancer stem cells. Nanomedicine (Lond) 11: 2565-2579, 2016.
25. Xie F, Zhang S, Liu J, Gong Z, Yang K, Zhang H, Lu Y, Zou H, Yu Y, Chen Y, et al: Codelivery of salinomycin and chloroquine by liposomes enables synergistic antitumor activity in vitro. Nanomedicine (Lond) 11: 1831-1846, 2016.
26. Wang M, Xie F, Wen X, Chen H, Zhang H, Liu J, Zhang H, Zou H, Yu Y, Chen Y, et al: Therapeutic PEG-ceramide nanomicelles synergize with salinomycin to target both liver cancer cells and cancer stem cells. Nanomedicine (Lond) 12: 1025-1042, 2017.
27. Naujokat C and Steinhart R: Salinomycin as a drug for targeting human cancer stem cells. J Biomed Biotechnol 2012: 950658, 2012.
28. Gao J, Feng SS and Guo Y: Antibody engineering promotes nanomedicine for cancer treatment. Nanomedicine (Lond) 5: 1141-1145, 2010.
29. Mamot C, Ritschard R, Wicki A, Stehle G, Dieterle T, Bubendorf L, Hilker C, Deuster S, Herrmann R and Rochlitz C: Tolerability, safety, pharmacokinetics, and efficacy of doxorubicin-loaded anti-EGFR immunoliposomes in advanced solid tumours: A phase 1 dose-escalation study. Lancet Oncol 13: 1234-1241, 2012.
30. Miller K, Cortes J, Hurvitz SA, Krop IE, Tripathy D, Verma S, Riahi K, Reynolds JG, Wickham TJ, Molnar I, et al: HERMIONE: A randomized Phase 2 trial of MM-302 plus trastuzumab versus chemotherapy of physician's choice plus trastuzumab in patients with previously treated, anthracycline-naïve, HER2-positive, locally advanced/metastatic breast cancer. BMC Cancer 16: 352, 2016.